RESEARCH PAPER

Interaction between adherend plasticity and adhesive damage in metal/composite joints: application to bonded composite repair of metallic structures

N. Demmouche[1] · A. Albedah[2] · Sohail M. A. Khan Mohammed[2] · B. Bachir Bouiadjra[1,2] · F. Benyahia[2]

Abstract

The plasticity in the crack region is a great influence on the fatigue life of aircraft structures, and the adhesive damage has negative effects on the durability of bonded joints. In this paper, the interaction effect between the crack tip's plasticity and adhesive damage in a bonded composite repair of cracked metallic panels was analyzed using the three-dimensional finite element (FE) method. A damage criterion was implemented in the FE model to evaluate the damaged zone in the adhesive layer, and the plastic strain around the crack was extracted from the FE calculations. In this research, we have demonstrated that the applied load has very significant effects both on crack plasticity and adhesive damage, but the ductility of the repaired material has no significant effect on adhesive failure. Fatigue tests and SEM observations were performed to validate the numerical results.

Keywords Bonded composite repair · Plastic zone · Adhesive damage · Finite element method

1 Introduction

The use of bonded composite patches to repair damage and cracks in aircraft structural components has increased in recent years because of the many advantages composite materials offer in comparison to metals; for example, bonded composite patches are more efficient than metallic patches fastened mechanically [1–5]. The use of adhesive bonding reduces the stress concentrations and significantly reduces the risk of new crack initiation caused by additional fastener holes. In a bonded composite repair, the stresses around the crack tip are transferred to the composite patch throughout the adhesive layer. This transfer significantly reduces the stress intensity factor at the crack tip, which improves the fatigue behavior of repaired panels [6–10].

Several parameters affect the process of repairing damaged metal structures, including:

- The mechanical properties of the composite and adhesive [11–14]
- The geometrical properties of the composite and adhesive, which include the patch's shape, thickness (plies per number in the composite), shape, orientation of the plies, and adhesive thickness [15–17]

Other parameters during the bonding or after the repair process have significant effects on the repair's performance, including the thermal residual stresses attributable to the adhesive curing, the adhesive disbond attributable to fatigue loading, and the plastic strain generated in the metallic structure because of fatigue loading and crack propagation. Bachir Bouiadjra et al. [18] showed that the adhesive disbond reduces the fatigue life of repaired structures dramatically. Indeed, the adhesive disbond leads to a significant reduction in the stress intensity factor for repaired cracks that reduce the repair's performance. These authors showed that when the adhesive disbond propagates perpendicular to the crack, it degrades the

✉ B. Bachir Bouiadjra
bachirbou@yahoo.fr; belabbes.bachirbouiadjra@univ-sba.dz

[1] LMPM, Department of Mechanical Engineering, University of Sidi Bel Abbes, BP 89, Cité Ben M'hidi, 22000 Sidi Bel Abbes, Algeria

[2] Mechanical Engineering Department, College of Engineering, King Saud University, Riyadh, Saudi Arabia

repair's effectiveness considerably, while propagation of the adhesive disbond parallel to the crack does not have a significant effect on the repair's performance. Caminero et al. [19] monitored the disbond using the Lamb waves technique and showed that it has an approximately elliptical shape and propagates perpendicular to the crack.

Before patching with a thermal adhesive, the repaired area of the metallic structures must be heated to the adhesive's curing temperature. During cooling, the difference between the temperature of the aluminum structure and the composite (which have different coefficients of thermal expansion) generates residual stresses that leave the composite in compression and the metal in tension. Many researchers have analyzed the effects of the thermal residual stresses on repair efficiency. Mhamdia et al. [20] studied the effect of thermal residual stresses on the variations in the stress intensity factor at the tip of repaired cracks under thermo-mechanical loading. The researchers showed that optimizing the adhesive properties and patch sizes significantly reduces the negative effects of these residual stresses.

While the effects of the adhesive disbond and residual stresses have been studied widely, those of plasticity around the crack have not received much attention in the literature. Oudad et al. [21] showed that the presence of a composite patch considerably reduces the size of the plastic zone ahead of the crack. This reduction is very important in applying the concepts of linear fracture mechanics to repaired cracks. Albedah et al. [22] conducted an experimental study on the effect of changes in load amplitude on the fatigue life of cracked Al plates repaired with a composite patch. They showed that the change in the fatigue load amplitude from a high to a low load block has a retarding effect on crack propagation. However, this effect is attenuated when the crack is patched. This behavior was explained by the fact that patching the crack reduces the plasticity around it, which leads to a reduction in the stress transfer between the repaired structure and the composite patch.

In this study, the finite element (FE) method was used to analyze the interaction effect between the plasticity at the tip of a crack repaired with a bonded composite patch and adhesive failure. The damage zone theory was used to predict adhesive failure. This analysis helps us to evaluate the performance of repairs.

2 FE and damage models

Geometrical models consisted of $150 \times 50 \times 2$-mm V notch plates in both aluminum alloys 2024 T3 and 7075 T6. The geometrical characteristics of the notch were depth = 6 mm and angle = 60° (see Fig. 1). A crack that initiated from the notch tip was assumed to exist in the aluminum plate. Unidirectional $50 \times 50 \times 1.5$-mm carbon/epoxy patches were
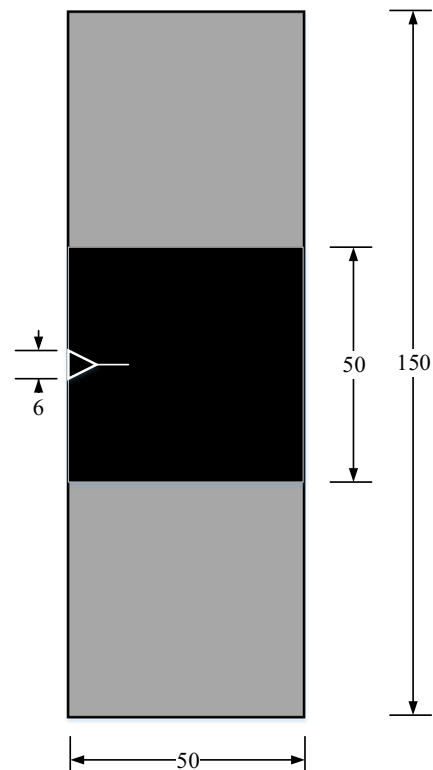

Fig. 1 Geometrical model

bonded to the cracked aluminum plate with Araldite epoxy adhesive, such that the lay-up principal direction was perpendicular to the loading direction, as shown in Fig. 1. The plate was subjected to a uniaxial load of amplitude $\sigma = 70$ and 200 MPa.

The FE tool ANSYS was used in this study. The FE model consisted of three subsections to model the cracked plate, adhesive, and composite patch. Because of its symmetry, only one half of the repaired plate was considered. The specimen, adhesive, and composite patch were modeled separately with the same exact mesh to maintain the bandwidth permitted. Both the 2024 T3 and 7075 T6 aluminum panels and the adhesive were considered elastic-plastic materials. The composite patch was considered an elastic-orthotropic material because the matrix (epoxy) is a thermosetting resin and the carbon fiber is a very hard material; in addition, the carbon/epoxy composite has three orthogonal planes of symmetry. The elements of the plate, adhesive, and composite patch were connected appropriately by merging the nodes on the contact surface. This is possible only by maintaining the same mesh for each. The elastic properties of the different materials are given in Table 1. The stress-strain curves of the two aluminum alloys are presented in Figs. 2 and 3 shows that of the Araldite 2015 [23].

To account for the material non-linearity in the FE model, a general static "STEP" was conducted. The material non-linearity model is based on Von-Mises combined with
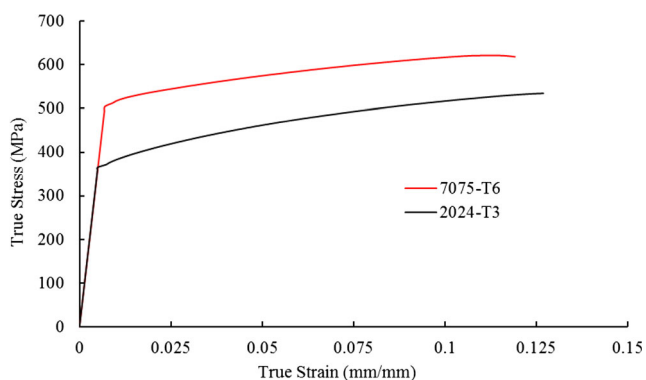
Table 1 Mechanical properties of different materials

Properties	Material			
	Al 7075 T6	Al 2024 T3	Carbon/epoxy	Adhesive (Araldite)
Longitudinal Young's modulus (GPa)	71.7	72.4	130	2.52
Transversal Young's modulus (GPa)	71.7	72.4	9	2.52
Longitudinal Poisson ratio	0.33	0.33	0.33	0.36
Transversal Poisson ratio	0.33	0.33	0.03	0.36
Hardness (HV)	39.1	29.5	–	–
Elongation at break (%)	10	18	–	–
Shear modulus (GPa)	28	26.9		0.954
Yield Strength (MPa)	503	370		

incremental plasticity theory as a plasticity criterion. The non-linear FE equations were solved using the Newton-Raphson iterative method in which the number of steps was limited to 100, with an incremental size range between 10^{-5} and 1, while the J integral along the curved front of the surface crack in three dimensions was computed using the domain-integral approach. Figure 4 shows the mesh of the specimen overall and mesh refinement in the crack's tip region.

The damage zone theory was used to predict adhesive failure [24], which is reached when the maximum principal strain in the material reaches the ultimate principal strain. The ultimate strain was defined for each failure criterion and the corresponding damage zone size at failure was determined. For the Araldite epoxy adhesive, the damage zone was defined as an area in which the strain exceeded the ultimate strain of 7.11% [23] (see Fig. 3). Under the damage zone theory, we assumed that the adhesive joint fails when the damage zone reaches a certain reference value. The damage zone ratio, D_R, is defined as follows:

$$D_R = \frac{\sum A_i}{lw} \tag{1}$$

A_i is the area over which the equivalent strain exceeds 7.15%, l is the adhesive length, and w is the adhesive width. The critical value of the D_R is 0.2474, which corresponds to the total failure of the adhesive layer [24].

3 Experimental setup

Following the standard ASTM E8, quasi-static tensile experiments were performed on both Al 2024 T3 and 7075 T6 samples at room temperature at a strain rate of $10{-}1\ \mathrm{s}^{-1}$ on an electro-mechanical Instron 5984 universal testing machine, and the strains obtained from the strain gauge were recorded on a strain indicator. The load obtained from the Instron load transducer was used to calculate the stress. The stress-strain diagrams obtained for the two materials are presented in Fig. 2. As the figure shows, the values of Young's modulus and yield strength were $E = 72.4$ GPa and 71.7 GPa, and the yield stress = 370 MPa and 503 MPa for Al 2024 T3 and Al 7075 T6, respectively.

To validate the numerical results of this research, we conducted fatigue tests employing the Servo hydraulic fatigue machine (Instron, type 8801—100 kN) on specimens of unrepaired aluminum alloys Al 2024 T3 and Al 7075 T6, and those repaired with a bonded composite patch, V-notched tension (SENT) according to ASTM E647 standards. The patches were made of unidirectional carbon/epoxy prepregs with eight unidirectional layers cured at 1200 °C for

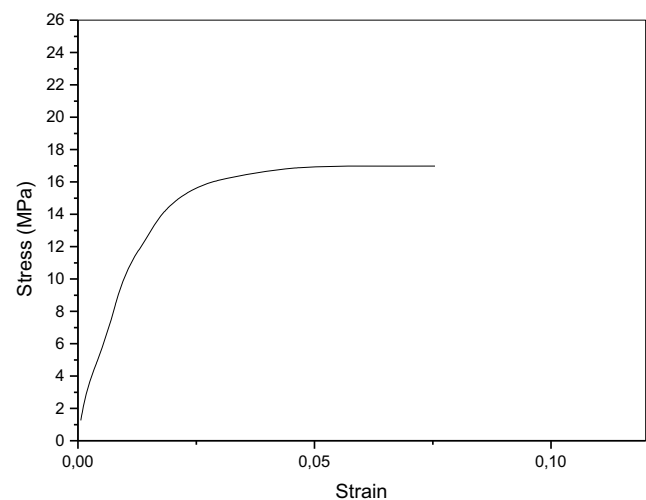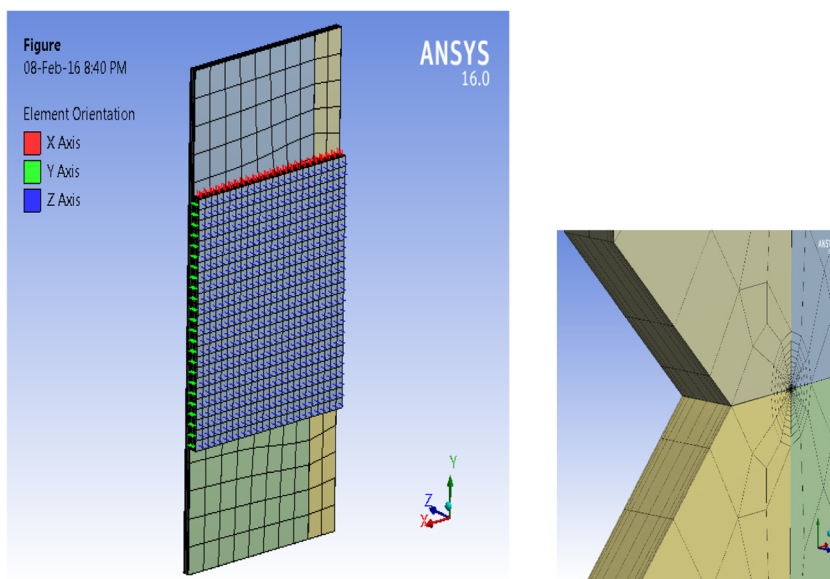**Fig. 2** Stress-strain curves of the Al 2024 T3 and Al 7075 T6

Fig. 3 Stress-Strain curve of the Araldite 2015 epoxy adhesive [23]

Fig. 4 Typical mesh model of the patched plate

90 min. The patch and the repaired plate were bonded with Araldite 2015 structural epoxy adhesive. The fatigue loading conditions were maximal stress $\sigma_{max} = 70$ MPa and the stress ratio was $R = 0.1$. The cracks were monitored with a high-resolution digital camera, and the fatigue life curves ($N = f(a)$) from the fatigue tests were plotted. Observations of the failed specimens after fatigue tests were performed with a scanning electronic microscope (SEM) to analyze the fracture surfaces.

4 Results and discussion

This study was conducted to analyze numerically the simultaneous effects of the plasticity and adhesive failure on the efficiency of the bonded composite repair of aircraft structures. The analysis was performed for the two main aluminum alloys used for aircraft structures: 2024 T3 and 7075 T6. Two different applied loads were chosen for this analysis: 70 MPa and 210 MPa (1/5 and 3/5 of the yield stress of the Al 2024 T3).

4.1 Applied load of 70 MPa

Figure 5 presents the variations in the plastic zone radius (r_p) as a function of the crack length for unrepaired plates in the two aluminum alloys. The applied stress was 70 MPa. This figure makes it clear that the r_p increased as the crack propagated and grew exponentially as a function of the crack length. These observations were valid for both alloys. The growth in the plastic zone area occurred because of the increased plastic strain around the crack tip as the crack propagates. However, Fig. 5 shows that the Al 2024 T3 had a higher r_p compared to

the 7075 T6, particularly when the crack's length exceeded 10 mm. These results are as expected, as Al 2024 T3 exhibits higher ductility compared to Al 7075 T6.

Figure 6 illustrates the variations in the r_p as a function of the crack length for plates repaired under an applied stress of 70 MPa. The r_p exhibited an asymptotic tendency when the crack propagated, which indicates that it becomes independent of the crack's length in the presence of the composite patch. On the other hand, when the results in Figs. 5 and 6 are compared, we can see that the composite patch reduced the r_p greatly. For example, for $a = 25$ mm, the r_p equals 8.3 mm for the unrepaired Al 2024 T3 plate and 4.2 mm for the Al 7075 T6. This radius decreased to 0.35 mm for the repaired Al 2024 T3 aluminum plate and to 0.15 mm for the repaired Al 7075 T6 plate. Thus, the r_p decreased by 26 times for Al 2024 T3 and 28 times for Al 7075 T6. Accordingly, we can deduce
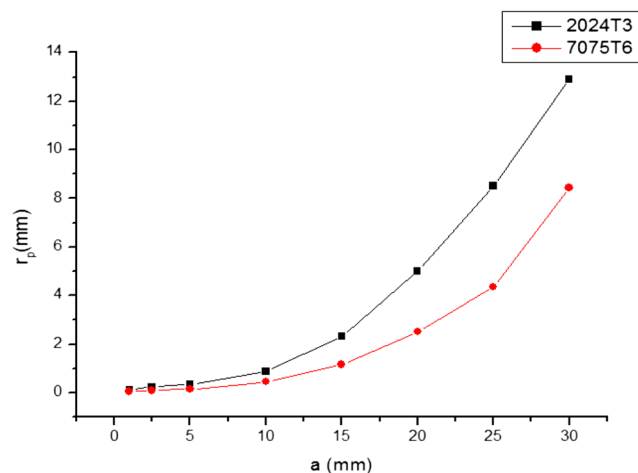

Fig. 5 Plastic zone radius vs crack length for unrepaired plates under $\sigma = 70$ MPa
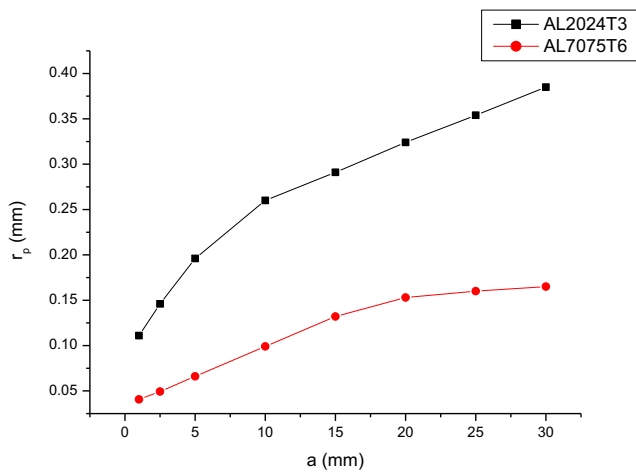
Fig. 6 Plastic zone radius vs crack length for repaired plates under $\sigma = 70$ MPa

that the composite patch reduced the rate of reduction in the plastic zone almost equally for the two aluminums alloys. This reduction is attributable to the load transfer between the repaired plate and the composite patch. This transfer attenuates the stress level around the crack tip and consequently reduces the plastic strain in this region.

To validate the numerical results, we present the experimental fatigue life curves of these two alloys and the SEM observations of their fracture surfaces in the unrepaired and repaired cases. Figure 7 presents the crack length as a function of the fatigue cycle number (N) for unrepaired specimens of the two aluminum alloys. The figure shows that the fatigue life of Al 2024 T3 was double that for Al 7075 T6. This indicates that increased ductility improves the fatigue tensile strength, which is consistent with the numerical results that showed a higher r_p for the Al 2024 T3 aluminum alloy. Figure 8a, b presents the SEM observations of fracture surfaces of unrepaired specimens of both Al 2024 T3 and Al 7075 T6.
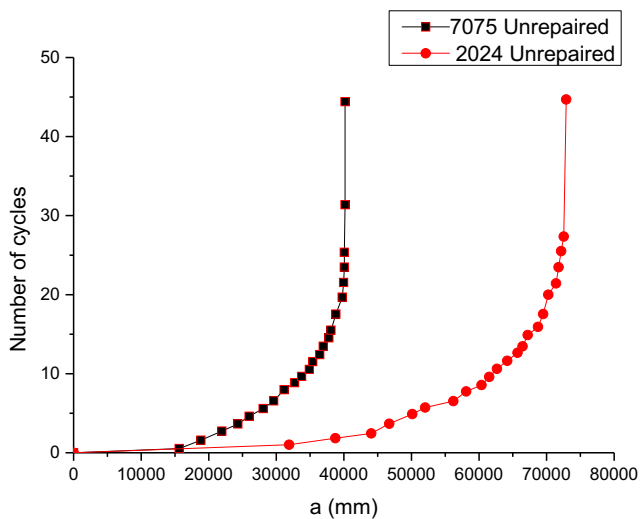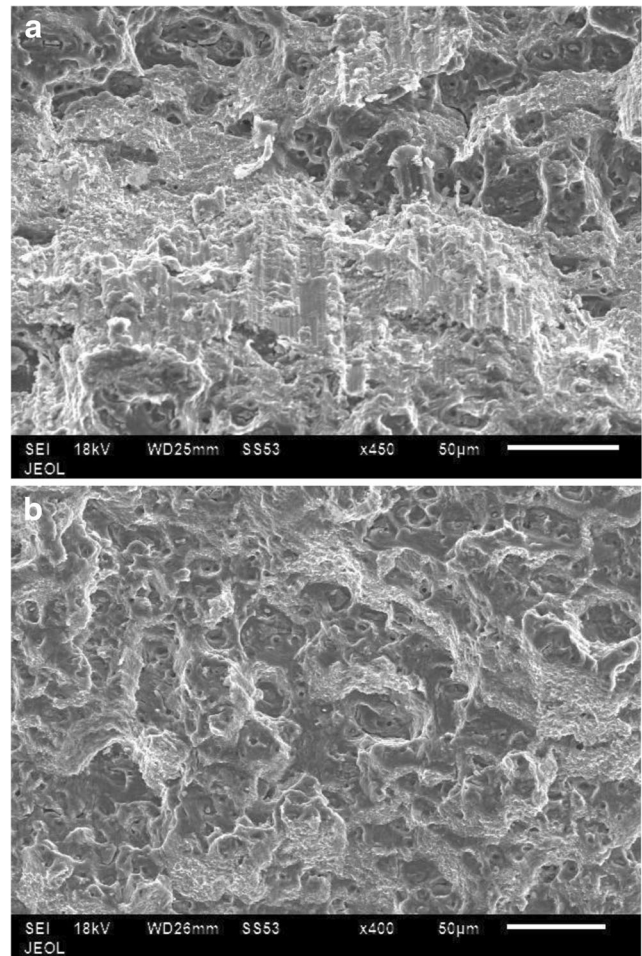

Fig. 7 Fatigue life curves for unrepaired specimens

Fig. 8 SEM observation of failed unrepaired specimens. **a** Al 2024 T3. **b** Al 7075 T6

The observations were conducted on the extreme part of the specimens where total failure occurred. We noted that the fractures differed between the two alloys (ductile and brittle). The ductile fracture is characterized by dimples and the brittle by pseudo-cleavage. Brittle fractures dominated in the Al 2024 T3, as the proportion of cavities was greater. However, there was a balance between the two fracture types.

Figure 9 presents the fatigue life curves of repaired specimens of the two alloys under fatigue loading at a constant amplitude of 70 MPa and a stress ratio of 0.1. We determined that the fatigue life increased greatly after patch bonding for both alloys. The composite repair increased the residual fatigue life, which confirmed the numerical results in Figs. 5 and 6. The reduction of the plastic zone shown in the numerical results is attributable to the stress transfer from the repaired plate to the composite patch throughout the adhesive layer. This stress transfer hinders the growth of the crack after patch bonding, and thus the composite patch increases the fatigue life. Figure 10a, b presents the SEM observations of the fracture surfaces of failed repaired specimens in the two alloys. From these figures, we can see that the fracture in repaired
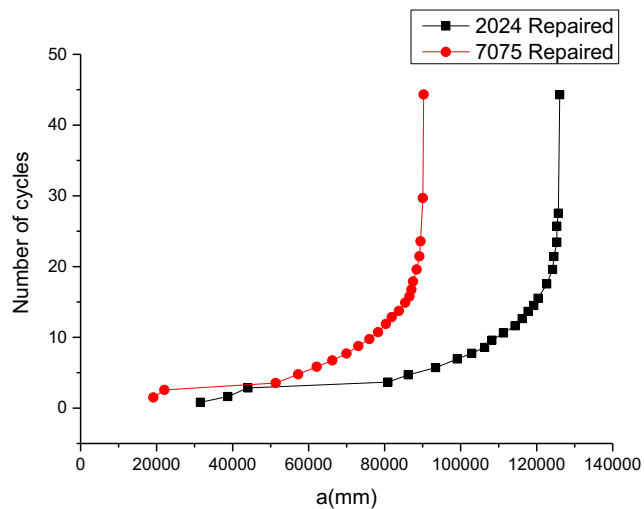
Fig. 9 Fatigue life curves of repaired specimens

specimens was largely brittle for both alloys. In the case of the Al 2024 T3, some cavities were visible, but fractures with pseudo-cleavage predominated, while for the Al 7075 T6 the fractures were completely brittle.
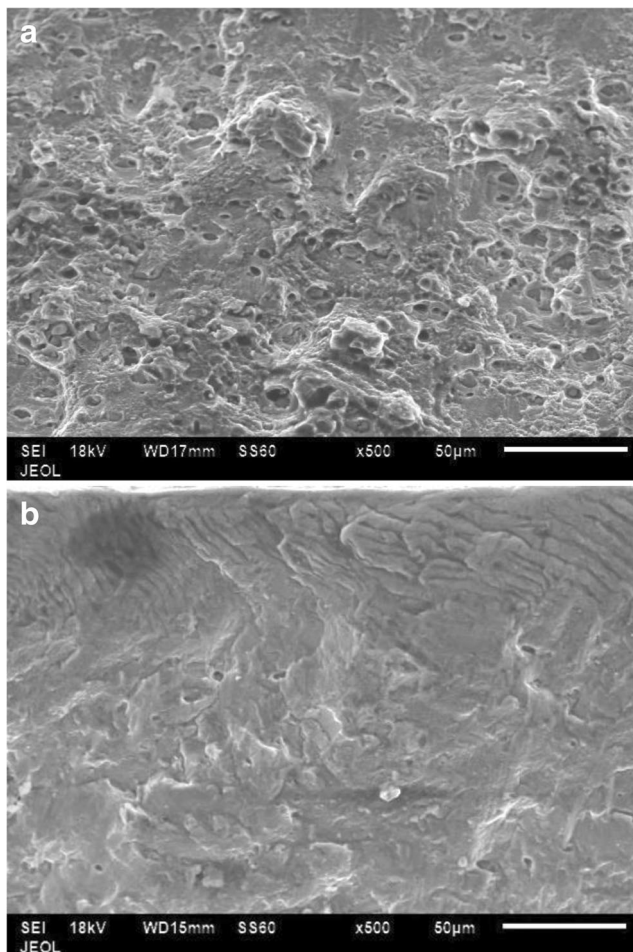

Fig. 10 SEM observations of failed repaired specimens. **a** Al 2024 T3. **b** Al 7075 T6

Figure 11 shows the plot of the D_R against the crack size for the two alloys under an applied stress of 70 MPa. The D_R increased linearly with crack propagation for the two Al alloys, but remained well below the critical value of 0.2474 regardless of the alloy repaired. Thus, we can deduce that the risk of adhesion failure is low with an applied load of 70 MPa. On the other hand, in Fig. 11, the two Al alloys had approximately the same D_R independently of the crack's size, which confirms that the risk of adhesive failure does not depend on the material ductility but instead exclusively on the level of the applied stress. Figures 12 and 13 confirm this conclusion. These figures show the damaged zone in the adhesive for patched Al 2024 T3 and Al 7075 T6, respectively, under an applied stress of 70 MPa. The damaged zone of the adhesive is clearly slightly greater for the Al 2024 T3 alloy.

These results are predictable because the level of the applied stress has no significant plasticity around the crack tip. In Figs. 12 and 13, we noted that, for an applied load of 70 MPa, the adhesive damage occurred principally above the cracked zone because of the high stress level around this zone. The cyclic loading can lead to increased adhesive damage and, consequently, to the total failure of the adhesive layer. It is clear in these figures that the damaged zone in the adhesive had an approximate elliptical shape, which is consistent with Caminero et al.'s experimental observations [19].

To better understand the interactions between the adhesive failure and the adherend plasticity in bonded composite repairs, we used an applied stress of 200 MPa, which corresponds to 57% of the yield stress of Al 2024 T3 and 40% of that of Al 7075 T6.

4.2 Applied stress of 200 MPa

To complete this study, it was imperative to repeat the previous calculations with an applied stress closer to the yield stress and therefore we chose the value of 200 MPa. Figure 14 presents the plot of the r_p around unrepaired cracks against the crack length. Crack propagation led to an extension of the
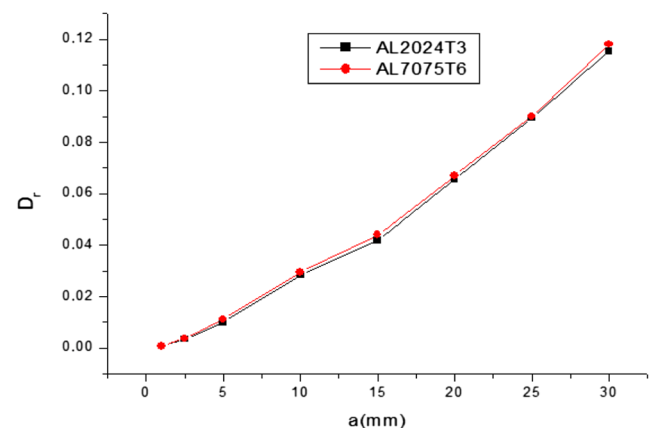

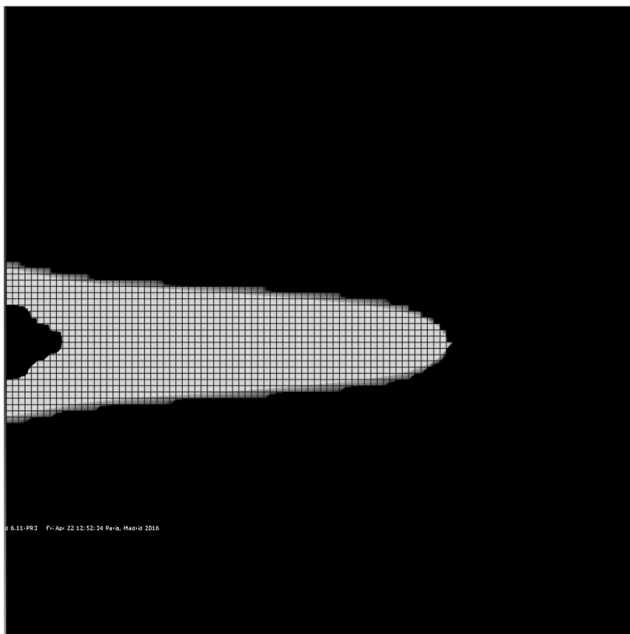**Fig. 11** Damage zone ratio vs crack length for $\sigma = 70$ MPa

Fig. 12 Damaged zone in the adhesive (in gray) for patched Al 2024 T3 specimen under $\sigma = 70$ MPa

plasticity around the crack, particularly under high loading. It is interesting to see that for this applied load (200 MPa), the r_p approximated the crack length value for the two Al alloys. Linear fracture mechanics approaches are not applicable in such cases.

Figure 15 presents the variation in r_p to the crack size for the two alloys under the applied stress of 200 MPa. The patch led to a significant drop in the r_p for both alloys, particularly Al 7075T6. For this alloy, the r_p was approximately 2 mm
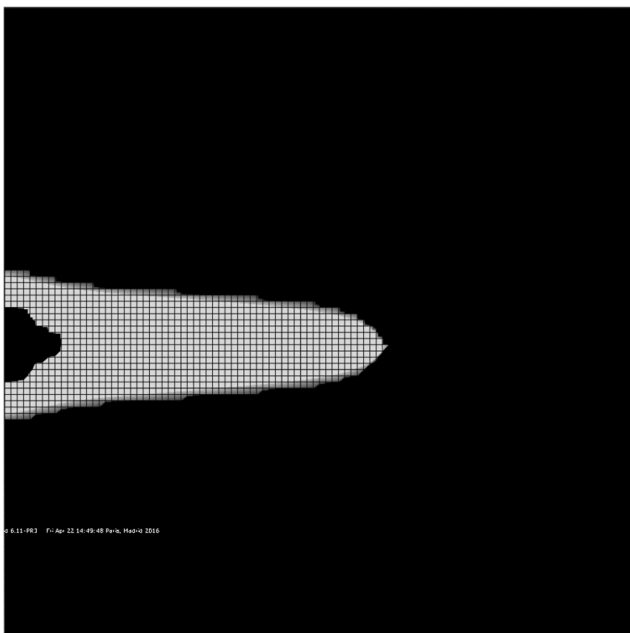

Fig. 13 Damaged zone in the adhesive (in gray) for patched Al 7075 T6 specimen under $\sigma = 70$ MPa
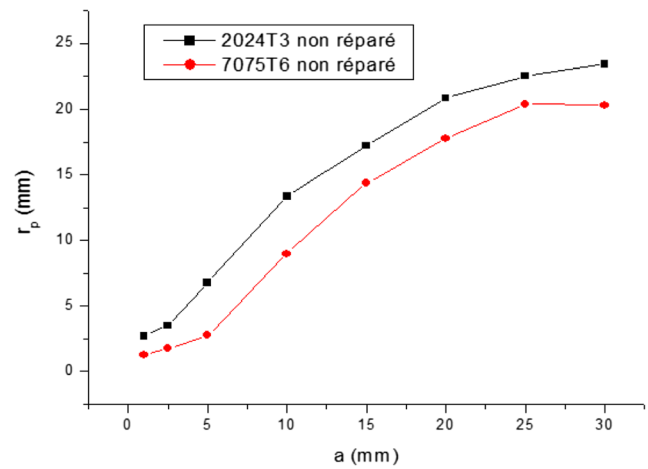

Fig. 14 Plastic zone radius vs crack length for unrepaired plates under $\sigma = 200$ MPa

when the crack size reached 30 mm ($r_p/a = 1/15$), while the ratio of r_p/a was approximately 1/5 for the Al 2024 T3. Thus, the composite reduces the plasticity of the repaired materials, but the rate of this reduction depends strongly on the material's ductility. Although the Al 2024 T3 demonstrated better fatigue resistance than 7075 T6, we can confirm that the material's ductility may affect the effectiveness of the repair if the applied load approximates the yield stress.

Figure 16 presents the variation in the D_R versus the crack length for the two alloys under an applied load of 200 MPa. The patched plates in the two alloys had exactly the same D_R regardless of the crack's size, which confirms that the risk of an adhesive debond is essentially independent of the material's ductility. However, we can see that for this applied stress (200 MPa), the D_R exceeded its critical value when the crack was longer than 10 mm. This indicates that the adhesive can fail completely when this crack length is exceeded. Failure of the adhesive layer causes the composite patch to detach from the repaired panel. To prevent this catastrophe, the repair
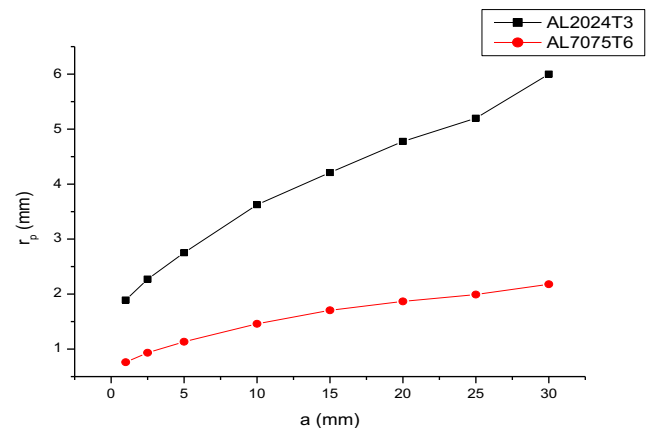

Fig. 15 Plastic zone radius vs crack length for repaired plates under $\sigma = 200$ MPa
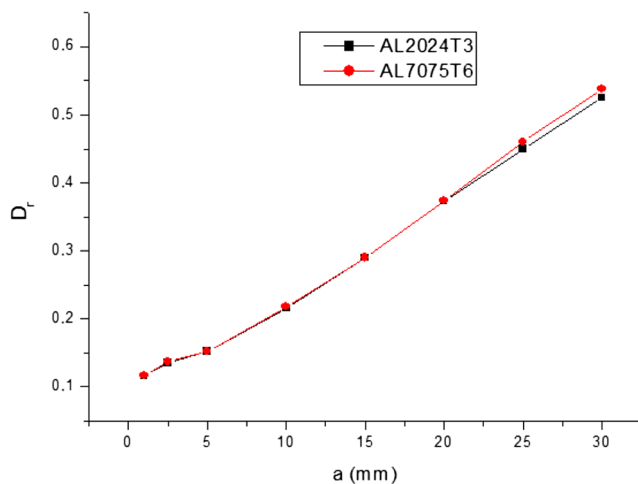
Fig. 16 Damage zone ratio vs crack length for $\sigma = 200$ MPa

designer should take precautions by choosing high-strength adhesives, increasing the bonded area, and preparing the bonded surface between the metal and the composite properly. To confirm the results above, Figs. 17 and 18 present the damaged zones in the adhesive for the two repaired aluminum alloys with an applied load of 200 MPa and a crack size of 30 mm, respectively. The figures show that the damaged zone in the adhesive (in gray) was very large, and typically exceeded 50% of the total bonded surface for the two aluminum alloys, which indicates that adhesive failure is unavoidable when the applied load increases excessively. Two zones of adhesive damage can be seen in Figs. 17 and 18: the first was located above the cracked zone and the second at the free
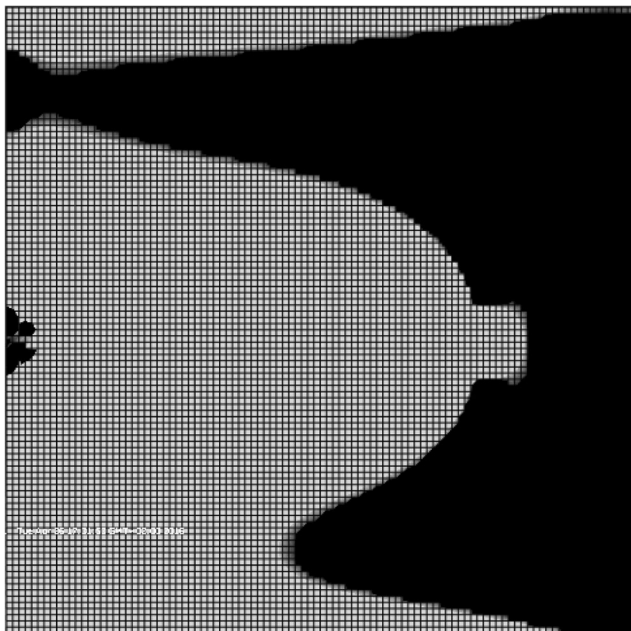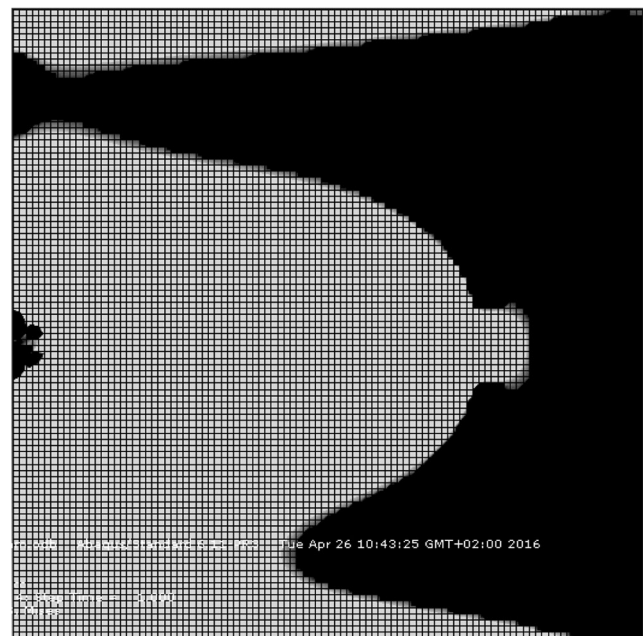

Fig. 18 Damaged zone in the adhesive (in gray) for the Al 7075 T6 under $\sigma = 200$ MPa

edges of the composite patch. The coalescence of these two zones leads inevitably to the total failure of the adhesive layer. The two figures also confirm that the propagation of the adhesive damage perpendicular to the crack was more significant because the zone of the high stresses around the crack tip increases when the applied stress or the crack's length increases. The increased stress around the crack tip leads to higher shear or peel stresses in the adhesive layer.

5 Conclusion

This study demonstrated that the presence of a composite patch reduced the plasticity around the crack front and the rate of this reduction depended on the applied load. The D_R in the adhesive layer also depended on the stress levels. A significantly high applied stress leads necessarily to an adhesive disbond between the composite patch and the repaired metallic panels. However, it was deduced from the results obtained that material ductility does not influence the D_R in the adhesive because, after repair, the two aluminum alloys exhibited the same D_R. It is recommended that designers of bonded composite patches choose an adhesive with high resistance and increase the bonded surface to reduce the D_R, which eventually minimizes the risk of adhesion failure.

Fig. 17 Damaged zone in the adhesive (in gray) for the Al 2024 T3 under $\sigma = 200$ MPa

References

1. Baker A, Gunnion AJ, Wang J, Chang P (2016) Advances in the proof test for certification of bonded repairs – Increasing the Technology Readiness Level. Int J Adhes Adhes 64:128–141

2. Hu W, Jones R, Kinloch AJ (2016) Computing the growth of naturally-occurring disbonds in adhesively-bonded patches to metallic structures. Eng Fract Mech 152:162–173

3. Albedah A, Berrahou M, Es-saheb M, Benyahia F, Bachir Bouiadjra B (2011) Gain estimation between double and single-bonded composite repairs for inclined cracks in aircraft structures. J Thermoplast Compos Mater 25:181–192

4. Aglan HA, Gan YX, Wang QY, Kehoe M (2012) Design guidelines for composite patches bonded to cracked aluminum substrates. J Adhes Sci Technol 16:197–211

5. Khan SM, Benyahia F, Bachir Bouiadjra B, Albedah A (2014) Analysis and repair of crack growth emanating from V-notch under stepped variable fatigue loading. Procedia Eng 74:151–156

6. Aakkula J, Saarela O (2014) An experimental study on the fatigue performance of CFRP and BFRP repaired aluminium plates. Compos Struct 118:589–599

7. Ouinas D, hebbar A (2010) Full-width disbonding effect on repaired cracks in structural panels with bonded composite patches. J Thermoplast Compos Mater 23:401–412

8. Schubbe JJ, Bolstad SH, Reyes S (2016) Fatigue crack growth behavior of aerospace and ship-grade aluminum repaired with composite patches in a corrosive environment. Compos Struct 144:44–56

9. Baker AA (2011) A proposed approach for certification of bonded composite repair to flight-critical airframe structure. Appl Compos Mater 18:337–369

10. Ahn JS, Basu PK, Woo KS (2010) Analysis of cracked aluminum plates with one-sided patch repair using p-convergent layered model. Finite Elem Anal Des 46:438–448

11. Benyahia F, Albedah A, Bouiadjra BAB (2014) Elliptical and circular bonded composite repair under mechanical and thermal loading in aircraft structures. Mater Res 17:1219–1225

12. Baker A, Rajic N, Davis C (2009) Towards a practical structural health monitoring technology for patched cracks in aircraft structure. Compos A: Appl Sci Manuf 40:1340–1352

13. Chung HK, Yang WH (2003) Mixed-mode fatigue crack growth in aluminum plates with composite patches. Int J Fatigue 25:325–333

14. Fari Bouanani M, Benyahia F, Albedah A, Aid A, Bachir Bouiadjra B, Belhouari M, Achour T (2013) Analysis of the adhesive failure in bonded composite repair of aircraft structures using modified damage zone theory. Mater Des 50:433–439

15. Mall S, Schubbe J (2009) Bonded composite patch geometry effects on fatigue crack growth in thin and thick aluminum panels. Struct Longev 2:25–48

16. Riccio A, Di Felice G, Scaramuzzino F, Sellitto A (2014) A practical tool for the preliminary design of bonded composite repairs. Appl Compos Mater 21:495–509

17. Brighenti R, Carpinteri A, Vantadori S (2006) A genetic algorithm applied to optimisation of patch repair for cracked plates. Comput Methods Appl Mech Eng 196:466–475

18. Bachir Bouiadjra B, Oudad W, Albedah A, Benyahia F, Belhouari M (2012) Effects of the adhesive disband on the performances of bonded composite repairs in aircraft structures. Mater Des 37:89–95

19. Caminero MA, Pavlopoulou S, Lopez-Pedrosa M, Nicolaisson BG, Pinna C, Soutis C (2013) Analysis of adhesively bonded repairs in composite: damage detection and prognosis. Compos Struct 95:500–517

20. Mhamdia R, Bachir Bouiadjra B, Serier B, Oudad W, Touzain S, Feaugas X (2012) Stress intensity factor for repaired crack with bonded composite patch under thermo-mechanical loading. J Reinf Plast Compos 30:416–424

21. Oudad W, Bachir Bouiadjra B, Belhouari M, Touzain S, Feaugas X (2009) Analysis of the plastic zone size ahead of repaired cracks with bonded composite patch of metallic aircraft structures. Comput Mater Sci 46:950–954

22. Albedah A, Khan SMA, Benyahia F, Bachir Bouiadjra B (2016) Effect of load amplitude change on the fatigue life of cracked Al plate repaired with composite patch. Int J Fatigue 88:1–9

23. Da Silva Lucas FM, Da Silva RAM, Chousal JAG, Pinto AMG (2008) Alternative methods to measure the adhesive shear displacement in the thick adherend shear test. J Adhes Sci Technol 22:15–29

24. Ban C-S, Lee Y-H, Choi J-H, Kweon J-H (2008) Strength prediction of adhesive joints using the modified damage zone theory. Compos Struct 86:96–100